

Fabrication of high frequency nanometer scale mechanical resonators from bulk Si crystals

A. N. Cleland^{a)} and M. L. Roukes

Condensed Matter Physics 114-36, California Institute of Technology, Pasadena, California 91125

(Received 21 June 1996; accepted 22 August 1996)

We report on a method to fabricate nanometer scale mechanical structures from bulk, single-crystal Si substrates. A technique developed previously required more complex fabrication methods and an undercut step using wet chemical processing. Our method does not require low pressure chemical vapor deposition of intermediate masking layers, and the final step in the processing uses a dry etch technique, avoiding the difficulties encountered from surface tension effects when wet processing mechanically delicate or large aspect ratio structures. Using this technique, we demonstrate fabrication of a mechanical resonator with a fundamental resonance frequency of 70.72 MHz and a quality factor of 2×10^4 . © 1996 American Institute of Physics. [S0003-6951(96)04144-7]

The combination of electron beam lithography and Si micromachining techniques makes it possible to fabricate submicron mechanical structures from single crystal substrates. Structures can be fabricated with fundamental mechanical resonance frequencies reaching into the microwave frequency bands, and can be made small enough that it is statistically unlikely that there are any crystalline defects contained within the structure. Such structures should exhibit very high quality factors and other mechanical properties that reflect the true nature of the material, such as large breaking stress. Elsewhere we have shown that such devices can be used in a new class of particle and energy sensors due to their very small mass, small size, high operating frequencies, and sensitivity to external conditions.¹ Furthermore, a resonator with a fundamental mechanical resonance frequency of a few times 10^9 Hz can be fabricated; this could exhibit macroscopic quantum effects at dilution refrigerator temperatures and might display interesting interactions with thermal phonons with the same range of frequencies.¹

Other authors have reported recipes for fabricating submicron suspended Si structures.^{2,3} These recipes are somewhat more complicated and require more extensive processing equipment than the method we describe here. The final undercut step of the suspended structures is performed in our recipe by using a dry etch process, which avoids potential damage due to surface tension encountered in wet etch processes. We first describe the method used to fabricate suspended structures, and then describe the method used to measure the resonance properties of simple doubly clamped beams and show data for one such structure.

We used $\langle 100 \rangle$ orientation, nominally undoped *n*-type Si wafers with a resistivity at 298 K of $>1000 \Omega \text{ cm}$. The substrates were cleaned, and on them a $1 \mu\text{m}$ SiO_2 layer was grown by pyrogenic steam oxidation for 1 h at 1100°C , with O_2 flowing at 0.4 scfm through water at 95°C ; this oxide layer serves as a mask for the isotropic reactive ion etching (RIE) of the Si substrate, the step that undercuts the suspended structures.

Large area contact pads were defined by optical lithography. A 100-nm-thick layer of Ni was rf sputtered onto a

lift-off pattern, and the photoresist removed by soaking in acetone.

We next deposited a polymethyl methacrylate (PMMA) bilayer on the oxidized substrates, with a 400-nm-thick underlayer of 496 KD PMMA and a 100-nm-thick overlayer of 950 KD PMMA. We patterned the bilayer by electron beam lithography with a 40 kV accelerating voltage and a dose of $350 \mu\text{C}/\text{cm}^2$. A 100-nm-thick layer of Ni was then rf sputter deposited onto the bilayer and then lifted off; the substrates then had the appearance of that shown in cross section in Fig. 1(a).

The pattern in the metal mask was transferred to the oxide layer beneath it by anisotropic RIE in a parallel plate reactor⁴ that has a 6-in.-diam cathode, a 4 in. anode-to-cathode spacing, and operates at 13.56 MHz. The cathode plate is water cooled to a little below room temperature. The etch chamber is oil diffusion pumped, and was always pumped to less than 2×10^{-5} Torr. For oxide etching, we used C_2F_6 flowing at 5 sccm with an indicated chamber pressure of 60 mTorr. The chamber pressure was measured by a thermocouple-type gauge.⁵ We used a rf power of 50 W, developing a plasma voltage of 280 V to the cathode of the reactor. The etch rate of SiO_2 in these conditions was 180–210 nm/min, and was stopped by timing the etch duration; we found that C_2F_6 did not etch Si at a noticeable rate, so the timing was not critical. The sidewalls in the patterned oxide were quite vertical, with an angle at most 5° from normal. At this point, the substrates had the appearance of that shown in Fig. 1(b).

After removing the substrates for inspection, they were returned to the RIE chamber for anisotropic etching of the Si.

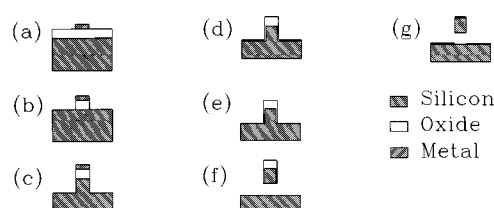


FIG. 1. (a)–(g) Schematic diagrams of the processing steps to generate suspended Si structures. The steps are as described.

^{a)}Electronic mail: cleland@cco.caltech.edu

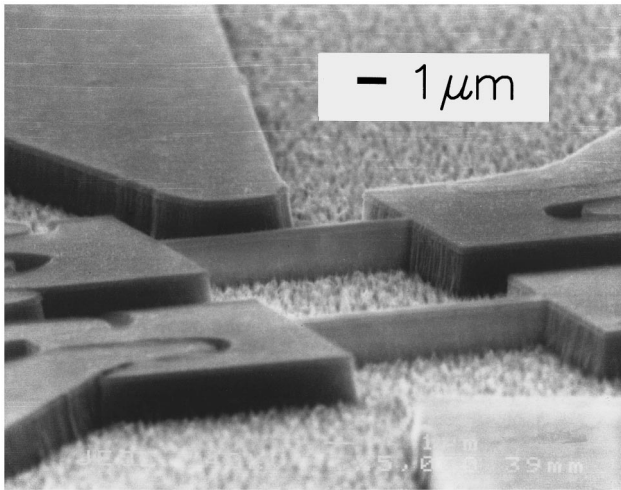


FIG. 2. SEM micrograph of the structures following the anisotropic Si etch.

We used a combination of NF_3 and CCl_2F_2 , each flowing at 5 sccm with a chamber pressure of 30 mTorr; rf power was 150 W, with a plasma voltage of 420 V. The etch rate for Si was found to be 1100 nm/min, with quite vertical sidewalls. At this point the structures were as shown in Fig. 1(c); a scanning electron microscope (SEM) micrograph of these structures is shown in Fig. 2. The Ni mask was removed by wet chemical etching and rinsing in de-ionized (DI) water. We then grew a sidewall oxide mask by pyrogenic oxidation at 1000 °C for 20 min; see Fig. 1(d).

In order to remove the oxide layer on the base surface of the etched structure, the substrates were placed in the RIE chamber and etched using the anisotropic SiO_2 recipe; the etch time was 15 min, somewhat overetching to ensure that all the base layer SiO_2 was removed.

At this point, the substrates had vertical ribs of single-crystal Si, with a thick oxide layer on the upper surface and a thin sidewall oxide on the vertical sidewalls; see Fig. 1(e). The vertical ribs were undercut in the final step, which was performed by RIE using pure NF_3 ; etching was masked by the remaining oxide layers. The NF_3 flow rate was 5 sccm, and the chamber pressure was 10 mTorr; rf power was 150 W, with a plasma voltage of 450 V. Because the etch rate of the top layer of SiO_2 was nearly as rapid as the etch rate of Si, timing in this step was critical. The structures were examined by SEM to ensure complete undercutting; see Fig. 3. Note that the undercut is not flat under the structure, but has a sharp point in the middle of the structure due to the isotropic nature of the etch; furthermore, we always observed some scalloping along the length of the structure, probably due to variations in oxidation of the exposed Si surface. Use of a non-RIE based etch⁶ might improve the surface quality.

At this point the structures were complete. The oxide layers could be removed by wet etching in hydrofluoric acid (48%) and rinsing in de-ionized water. Metallization was also performed at this point, by thermal evaporation of an adhesion layer of Cr (5–10 nm) followed by a layer of Au (100 nm). The undercutting of the entire structure ensured that the Au evaporated on the top of the structures was electrically isolated from that deposited in the base of the substrates; see Fig. 1(g). Typical isolation resistances, due to the

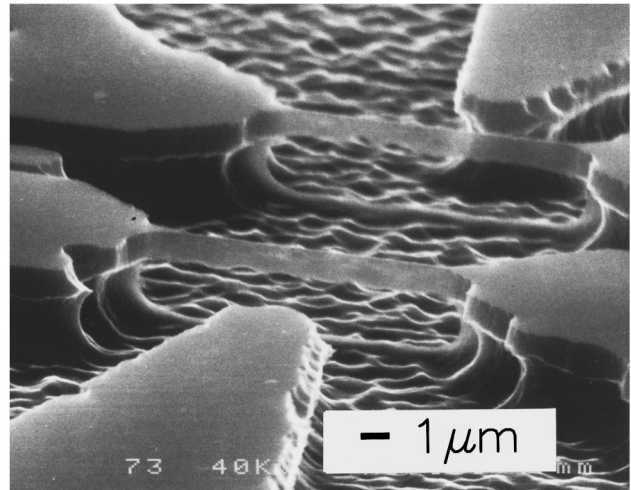


FIG. 3. SEM micrograph of an undercut Si beam, with length of 7.7 μm , width of 0.33 μm , and height of 0.8 μm . Some scalloping is visible along the bottom edge of the beam.

metal-Si Schottky barrier, were greater than 1 M Ω for bias voltages of less than about 0.1 V.

Using the technique described above, we have fabricated a number of suspended Si beams and have measured their resonance properties at a temperature of 4.2 K. The beams were placed in vacuum, with the long axis of the beam perpendicular to a magnetic field generated by a superconducting solenoid. Electrical connections were made by Au wire bonds to a chip carrier, and short lengths of Cu wire were soldered between the chip carrier and the center and the ground of a stainless steel coaxial cable that carried signals to the room temperature electronics. A network analyzer was used to drive an alternating current along the length of the beam and measure the response of the beam. The alternating current, transverse to the magnetic field, generates a Lorentz force that drives the beam transverse to its length and to the field direction. The motion of the beam then generates an electromotive force (EMF) along the length of the beam; the EMF is detected by the network analyzer. A schematic of the measurement setup is shown in Fig. 4. A similar technique has been used by other authors.⁷ Several authors have reported measurements on larger beams at lower frequencies performed using either electrostatic⁸ or optical⁹ detection, but these techniques do not extend easily to smaller structures at higher frequencies.

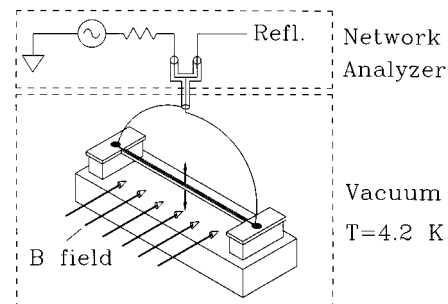


FIG. 4. Schematic illustration of the experimental setup used to measure the resonance properties of the Si structures.

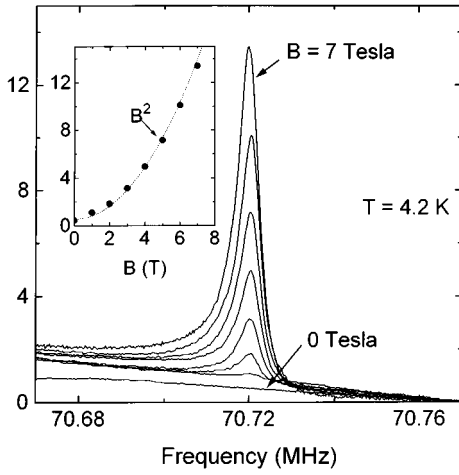


FIG. 5. Induced EMF as a function of drive frequency for the structure in Fig. 3. Magnetic field strength ranged from 0 to 7 T at a temperature of 4.2 K. Drive amplitude was 10 mV. Inset: Induced EMF at resonance as a function of field strength. The vertical axis has same units as the main plot.

These beams should have mechanical resonance frequencies ω_n as given by

$$\frac{\omega_n}{2\pi} = C_n \sqrt{\frac{E}{\rho}} \frac{w}{L^2}, \quad (1)$$

where E is Young's modulus, ρ is the density, w is the beam width in the direction of motion, and L is the beam length; the constants C_n , of order unity, depend on the mode number n and on the clamping conditions at the ends of the beam. If such a beam is driven by a force $F(\omega)$ near a resonance frequency ω_n , then to first order in the mode amplitude the beam responds as a harmonic oscillator and, assuming a damping term proportional to the beam velocity, the amplitude $u(\omega)$ should have a Lorentzian line shape given in

$$u(\omega) = \frac{F(\omega)/k_{\text{eff}}}{\sqrt{(\omega^2 - \omega_n^2)^2 - \omega^2 \omega_n^2 / Q^2}}, \quad (2)$$

where k_{eff} is the effective spring constant and Q is the quality factor. Note that in our system the force F depends linearly on the magnetic induction B , and the EMF generated by the motion is proportional to the product of B and the beam velocity du/dt , and should scale as B^2 .

We have measured the fundamental resonance frequencies of a number of beams with different geometries, with resonance frequencies ranging from 400 kHz to 120 MHz, and quality factors from about 10^3 to a few times 10^4 . In Fig. 5(a) we display the measured resonance of the beam shown in Fig. 3 that was measured for a range of magnetic fields from 0 to 7 T; the resonance frequency was 70.72 MHz, and the quality factor, determined by fitting a Lorentzian to the

resonance shape, was found to be about 1.8×10^4 . Shown in Fig. 5(b) is the peak height of the resonance measured as a function of the magnetic field induction; the induced EMF scales as the square of the field strength, as expected.

Note that the vertical scales of the plots in Fig. 5 cannot be interpreted to give beam displacements, as we do not know the exact coupling parameters of the beam to the coaxial cable used to transmit the radio-frequency signals. However, we estimate that the maximum displacement amplitudes for the data shown in Fig. 5 are a few nanometers. Larger drive currents were also used; they generated very noticeable divergences of the resonance shapes from the Lorentzian, as was expected from terms of higher order than the amplitude squared in the beam bending energy.

It would be of great interest to fabricate a 1 GHz resonant beam using this technique by simply reducing the length L of the beam by a factor of 4. However, this would reduce the signal-to-noise (S/N) ratio of the measurement technique by a factor of at least 64, and more if the Q is adversely affected by the reduction in aspect ratio L/w . We propose fabrication of a beam with dimensions $1.3 \times 0.15 \times 0.2 \mu\text{m}^3$, with an expected S/N reduction of about 10 if the Q remains the same. A reduction in the length and width of the beam of this order is fairly straightforward, while reducing the height would require very careful timing of the Si anisotropic etch. Use of laser end-point detection during RIE should make this feasible.

In conclusion, we report on a method for fabricating submicron single-crystal mechanical resonators that uses a single metal mask, two steps of thermal oxidation, and four steps of reactive ion etching to generate a suspended mechanical structure. We have also shown data taken on a radio frequency resonator at low temperatures, with a reasonably high quality factor. Work is in progress to fabricate resonators with higher fundamental resonance frequencies, and we are investigating methods to reach even higher quality factors.

The authors acknowledge Dr. Axel Scherer for many valuable conversations, and for use of his reactive ion etch system. This work was supported by ARPA under Contract No. DABT63-95-C-0112.

¹A. N. Cleland and M. L. Roukes (unpublished).

²S. C. Arney and N. C. MacDonald, *J. Vac. Sci. Technol. B* **6**, 341 (1988).

³J. Yao, S. Arney, and N. C. MacDonald, *J. Microelectromech. Sys.* **1**, 14 (1992).

⁴Materials Research Corp., Orangeburg, NY.

⁵Convectron gauge (series 275, Granville-Phillips Corp., Boulder, CO).

⁶H. F. Winters and J. W. Coburn, *Surf. Sci. Rep.* **14**, 161 (1992).

⁷D. S. Greywall *et al.*, *Phys. Rev. Lett.* **72**, 2992 (1994); D. S. Greywall, B. Yurke, P. A. Busch, and S. Arney, *Europhys. Lett.* **34**, 37 (1996).

⁸R. E. Mihailovich and N. C. MacDonald, *Sens. Actuators A* **50**, 199 (1995).

⁹J. D. Zook *et al.*, *Sens. Actuators A* **52**, 92 (1996); D. W. Burns *et al.*, *Sens. Actuators A* **48**, 179 (1995).